Polymorphic Behavior in Protein−Surfactant Mixtures: The Water−Bovine Serum Albumin−Sodium Taurodeoxycholate System

Barbara Orioni,[†] Mauro Roversi,[†] Camillo La Mesa,*[,†,‡] Fioretta Asaro,[§] Giorgio Pellizer,[§] and Gerardino D'Errico[||]

Dipartimento di Chimica and SOFT-INFM-CNR Research Center, Università "La Sapienza", P.le A. Moro 5, 00185 Roma, Italy, Dipartimento di Scienze Chimiche, Università degli Studi, Via L. Giorgeri 1, 34127 Trieste, Italy, and Dipartimento di Chimica, Università Federico II, Via Cintia, 80126 Napoli, Italy

Received: October 18, 2005; In Final Form: March 13, 2006

Mixtures containing water, bovine serum albumin (BSA), and sodium taurodeoxycholate (NaTDC), a component of the bile in mammals, have been investigated in a wide range of composition and pH. Depending on the concentration of both solutes and the pH, solutions, precipitates, and gels are formed. Under spontaneous pH conditions, the transport properties in dilute solutions indicate the occurrence of significant interactions between BSA and the surfactant. Conversely, acidic media favor the formation of nonsoluble protein−surfactant complexes, with subsequent precipitation. The nucleation kinetics of the protein−surfactant complexes in solid form and the related precipitation processes can be slow or fast, depending on the overall solute content and the mole ratio. At high concentrations, a gel, extending on both sides of the charge neutralization line, and two-phase regions are observed. Gels shrink in open air and swell in the presence of excess water. Depending on concentration and temperature, the gels transform from an essentially liquidlike behavior to that peculiar to true gels (when $G' \geq G''$). The thermal gelation threshold, the temperature above which $G' \geq G''$, depends on BSA and NaTDC content and is concomitant to moderate heat effects, inferred by differential scanning calorimetry (DSC). The above data also indicate that the protein thermal denaturation in the gel is shifted to higher temperatures compared to water. Such a stabilizing effect is presumably related to the occurrence of both electrostatic and hydrophobic interactions with NaTDC. Water self-diffusion in the gels is slightly slower than that in the bulk and poorly sensitive to composition: it is about 65% the value of neat H_2O in a wide concentration range, irrespective of the BSA, or NaTDC, concentration. A peculiar behavior is also observed in ^{23}Na longitudinal and transverse relaxation rates. The T_1 and T_2 values, measured at 105.75 MHz on BSA−NaTDC gels, indicate that the motions determining the NMR relaxation of the sodium ions in the hydration layer of the protein−surfactant aggregates are not slow, having frequencies comparable with the Larmor one. The above properties, especially the rheological and the spectroscopic ones, are important for understanding the behavior of gels based on protein−surfactant mixtures.

Introduction

The solution behavior of bile salts, essentially the glyco and tauro derivatives of the cholic, deoxycholic, and chenodeoxycholic acids, is relevant to fat adsorption and digestion processes in mammals.[1−3] Chemically, the bile salts (BS) are byproducts of the cholesterol pool.[4] They stabilize food suspoemulsions and adsorb at interfaces.[5] From such a point of view, they share many properties with normal surfactants. However, due to the presence of polar and nonpolar sides in the same planar molecule, their association features are peculiar compared to normal surfactants and strongly depend on concentration, ionic strength, and pH.[6−8] BS self-associate, forming micelle-like entities [9−11] (even if proper micelle formation has long been questioned)[12] and forming liquid crystalline phases.[13,14] The peculiar organization modes of BS units into micelle-like aggregates, gels, fibers, and liquid crystalline and solid phases[15] are quite different from the ones pertinent to most surfactants and lipids.[16]

In the intestinal pool, BS participate in the formation of mixed supramolecular aggregates with sterols, fatty acids, glycerides, and phospholipids.[17,18] The presence of other species, including proteins and their derivatives, and the physicochemical conditions in the intestinal duct (essentially pH and ionic strength) allow the formation of protein−surfactant complexes (PSC).[19,20] On these grounds, it is expected that ubiquitous proteins, such as albumins, may interact with BS. This hypothesis is supported by in vitro and in vivo investigation.[21,22]

The association between polymers, or proteins, and surfactants is explained in terms of a macromolecule centered binding approach, or a surfactant-based self-assembly one.[23] The latter has gotten general acceptance. The surfactant-based approach was fruitfully applied to systems where free micelles, well defined in size and shape, occur. It has been applied, for instance, to mixtures containing sodium dodecyl sulfate (SDS).[23] It can hardly be applied to bile acid salts, with their aggregates showing a (quasi)continuous variation in size and shape as a function of surfactant content.[24] In many aspects, the supramo-

* Corresponding author. Phone: +39-06-491694; +39-06-49913707. Fax: +39-06-490631. E-mail: camillo.lamesa@uniroma1.it.
[†] Dipartimento di Chimica, Università "La Sapienza".
[‡] SOFT-INFM-CNR Research Center, Università "La Sapienza".
[§] Università degli Studi.
[||] Università Federico II.

10.1021/jp055950r CCC: $33.50
Published on Web 05/26/2006

lecular association in bile acid salts can be explained in terms of a noncritical multimer concentration model[25] and implies that small micelles progressively evolve into large ones.[24] Hence, the surfactant-based self-assembly approach can be applied provided drastic approximations are introduced.

The mechanisms underlying the interactions between albumins and sodium taurodeoxycholate (NaTDC), or other bile acid salts, are presumably more complex than those occurring with *n*-alkyl chain surfactants or fatty acids. The latter substances enter the hydrophobic pockets of such proteins and/or interact electrostatically with specific binding sites. The binding of surfactants onto albumins is, generally, strongly cooperative. The relatively low values of BS binding constants onto albumins and other proteins are ascribed to their peculiar molecular structure. In fact, the K_{bind} values of BS onto albumins are about 2 orders of magnitude lower than those of synthetic surfactants, or fatty acids.[26]

Despite the fundamental and biomedical relevance of the above items, little information is available on the solution behavior of protein−surfactant systems (PSS), chemically related to human bile, under physiological or pathological conditions. Most physicochemical studies reported so far deal, essentially, with the BS solution behavior in the presence of sterols and/or lipids.[27−29] In this contribution, studies on the (partial) phase diagram of a ternary system composed by water, bovine serum albumin (BSA), and NaTDC are conducted.

Many effects are important in PSS, and a deeper understanding of the main factors controlling them is of fundamental significance. Presumably, pH affects the strength of protein−surfactant interactions (PSI). That is why efforts were performed in this work to determine its role in the phase diagram of the water−BSA−NaTDC system and in the formation of PS gels, when the mixtures contain proper amounts of BSA and BS.[30]

Gels containing proteins, polysaccharides, lipids, and/or natural surfactants are observed in a lot of biochemically relevant systems. They are assumed to be built up in terms of hierarchical self-assembly modes. For instance, structured layers are present at the gel−water interface.[31] Protein−surfactant gels have relevance in many problems connected with tissue engineering. The physical state and functions of the proteins in such matrixes are, presumably, different from those in the bulk. It can be useful, thus, to get information on the macroscopic physicochemical properties of the gel and on some properties pertinent to proteins in such matrixes.

To get a comprehensive view of significant aspects pertinent to biochemically relevant PSS is a formidable task, requiring the use of many ad hoc techniques. For these purposes, the partial phase behavior, the occurrence of a gel phase, and some precipitates in the water−BSA−NaTDC system were investigated, by combining information inferred from optical microscopy, ionic conductivity, scanning electron microscopy (SEM), differential scanning calorimetry (DSC), NMR self-diffusion and sodium relaxation, and rheological methods. Efforts shall be made to explain the observed properties occurring in the various phases of the water−BSA−NaTDC system and to get rational information as a basis for future fundamental work along this line.

Experimental Section

Materials. Fatty acid free (defatted) bovine serum albumin (BSA) was purchased from Sigma-Aldrich, lot no. 81K1554. The lyophilized protein powder was vacuum-dried and used as such. To minimize BSA exposure to light and moisture, the mixtures were stored in flame sealed glass ampules in the dark until use.

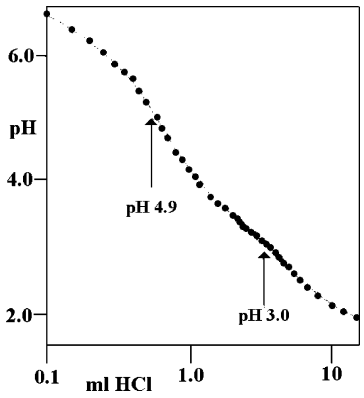

Figure 1. Potentiometric titration of 100 mL of a 1.00 wt % BSA solution with 0.1 M HCl, at 25.0 °C. pH values corresponding to the first and second inflection points are indicated by arrows.

The solution properties of BSA were controlled by density, viscosity, refractive index, potentiometric, and ionic conductivity methods, at 25 °C.[32−34] In freshly prepared solutions, the spontaneous pH of aqueous protein solutions is in the range 6.2−6.4, depending on BSA content. Potentiometric titration experiments, performed by adding proper amounts of HCl to aqueous BSA, indicate that the acid groups facing the outside of the protein can be roughly divided into two populations, having pK_a values of about 5.0 and 3.0, respectively (Figure 1). The former value is very close to the isoelectric point of defatted BSA (4.9).[35] Under spontaneous pH conditions, therefore, the protein has a slight excess of negative charges. Generally, 18 negative charges in excess face the outside of the protein when the pH is close to 6.5−7.0.[26]

NaTDC, Sigma Aldrich, was dissolved in hot absolute ethanol, filtered, and precipitated by the addition of cold acetone. The whole procedure was repeated twice, and the final product was vacuum-dried at 75 °C. The surfactant purity was checked from surface tension and electrical conductance. The critical concentration in water, inferred by surface tension, is in the range 3−4 mmol Kg^{-1}, at 25.0 °C, in good agreement with previous findings.[36]

HCl (0.1 M, Normex), ethanol, and acetone were of analytical purity, Sigma-Aldrich.

Water was filtered, doubly distilled over alkaline $KMnO_4$, deionized, and degassed. Its ionic conductivity, at 25 °C, is close to 1 μS cm^{-1}. When required, D_2O (Merck, 99.5 isotopic enrichment) was used on a mole fraction basis.

Mixture Preparation and Material Characterization. The aqueous solutions were prepared by weight and corrected for buoyancy. The samples were sealed in glass vials and kindly heated for 1 day in an air oven, under mild shaking, at 35 °C. In this way, the dissolution is relatively fast, even at high solute content. The samples in the vials were equilibrated in the dark at room temperature for several days, systematically controlled by visual inspection and optical microscopy until macroscopic equilibrium was deemed to be attained. Use of the above procedures avoids thermal and biological degradation of BSA. Samples to be investigated in open air (in rheological experiments, for instance) were used within 1 day, in the presence of water vapor; see below for details.

Mixtures at pH 5.0 and 3.0 were prepared by adjusting the solution acidity with 0.1 M HCl, under potentiometric control, by means of a Corning potentiometer, model 155. This procedure does not modify significantly the medium ionic strength, avoids using tris(hydroxymethyl)aminomethane (Tris)−HCl buffers, which have a non-negligible effect on the critical

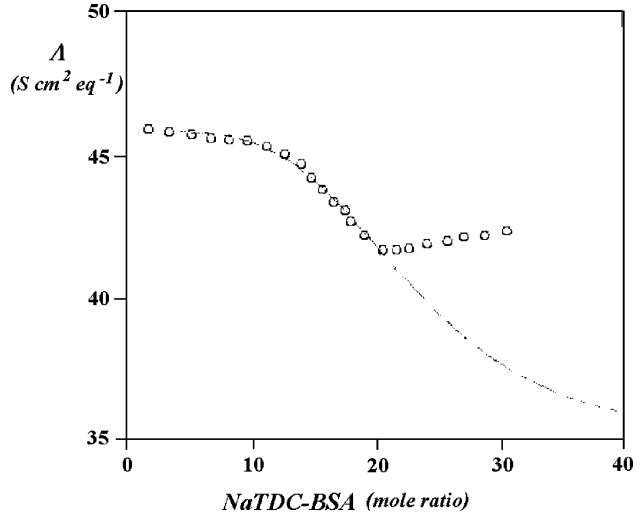

Figure 2. Equivalent conductance, Λ (S cm^2 eq^{-1}), versus the mole ratio of bile salt to albumin, at 25.00 °C and pH 6.4, for a 1.00 wt % BSA solution. The dotted line is the best fit of the data, calculated assuming the presence of 18 binding sites per BSA molecule. Departures from the above behavior indicate completion of binding and formation of free micelles.

micelle concentration (cmc) of surfactants,[37] and minimizes the competition between Cl^- and TDC^- ions toward the protein binding sites.[38]

Methods. *Ionic Conductivity.* A 6425 impedance bridge (Wayne-Kerr, Cambridge, USA) is used to perform the ionic conductivity measurements. The conductivity cell is located in an oil bath. The temperature, 25.000 ± 0.002 °C, is controlled by an A.S.L. platinum resistance thermometer. Addition of surfactant to the BSA solution was made through known amounts of proper water−BSA−NaTDC mixtures from a weight buret, under mild stirring.

Equivalent conductance values, Λ (S cm^2 eq^{-1}), were obtained from the specific ones, χ, by subtracting the contribution due to the solvent medium. Data relative to mixtures containing 1.00 wt % BSA are plotted versus the BSA/NaTDC mole ratio in Figure 2.

Rheology. The instrument is a stress controlled TA AR-1000 unit, working in the range 0.1−100 Hz. The rotor position, driven by an air flow, is controlled by an electronic apparatus. The cone-plate geometry was used. The temperature of the plate is controlled by a Peltier unit, operating between −10.0 and 99.9 °C with an accuracy of ±0.02 °C. Details on the unit setup, cone geometry, and measuring procedures are given elsewhere.[39−41] The composition was kept constant during the measurements by covering the gel and the operating unit by a wet paper cup. Macroscopically heterogeneous samples were not investigated.

The system response with respect to shear stress, σ, was controlled. This was done by selecting a linear viscoelastic regime, where both the elastic, G', and viscous, G'', components are constant and independent of σ[42] (Figure 3). Such a linear regime holds for σ values below 5.0 Pa and slightly depends on the gel composition. Its width was determined by stress-sweep measurements, under oscillatory conditions.

Measurements as a function of frequency, ω, at different temperatures were also performed at σ = 5.0 Pa. Some rheological data as a function of temperature are reported in Figure 4.

DSC Measurements. The DSC calorimeter is a Pyris Perkin-Elmer unit, working under N_2 gas flow, with a 2 μW sensitivity. Measurements were performed in the range 10−100 °C. The

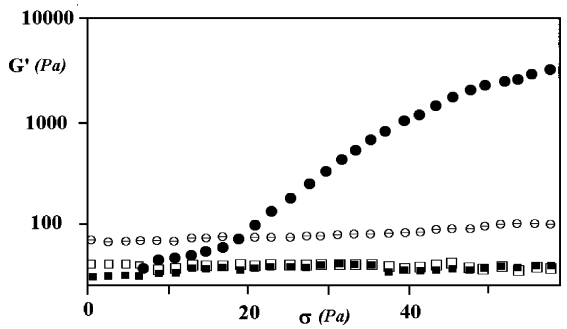

Figure 3. Dependence of G' (Pa) on the oscillation stress, σ (Pa), for a gel mixture containing 10.60 wt % BSA and 5.40 wt % NaTDC in water, at 25.0 (■), 35.0 (□), 45.0 (⊖), and 55.0 (●) °C. Errors on G' values are to within the symbol size. To avoid the overlapping of symbols, those at 35 °C have been drawn in a larger size.

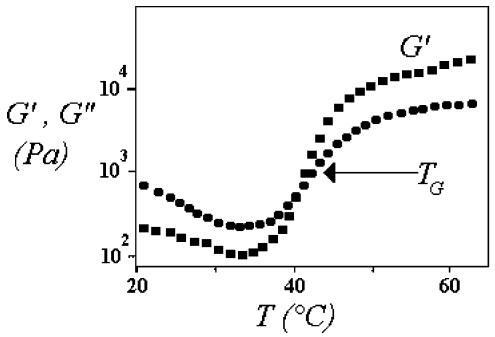

Figure 4. Semilogarithmic plot of G' and G'' (in Pa) vs temperature (°C), obtained by ramp experiments. The sample contains 12.40 wt % BSA and 8.25 wt % NaTDC. The thermal gelation threshold, indicated by an arrow, is the intersection point of G' and G'' curves. The experimental conditions are σ = 5.0 Pa, 1 °C min^{-1}, and 1.0 Hz.

scan rate (1.0−5.0 °C min^{-1}) depends on BSA, or NaTDC, content, sample consistency, and temperature. The sample mass is about 30 mg, the accuracy of transition temperatures, T_{tr}, is ±0.1 °C, and the errors on ΔH are ±2.0%. More details on the measuring procedures are given elsewhere.[43]

Visual Observation and Optical Microscopy. A Ceti Laborlux transmission microscope was used to determine the optical textures of the gels in white and polarized light.[44] The gels were stored at room temperature for some days. The gel viscosity is high, and no apparent material flow is observed in 2 weeks. The samples are stable, transparent, and yellowish. Their color intensity increases in proportion with BSA and NaTDC content. Before investigation, the samples were sheared between glass plates, to avoid inhomogeneities and bubbles. No finely dispersed particles or optical anisotropic textures were observed. No shear-induced formation of anisotropic textures could be detected.

Gel Swelling and Dehydration. Samples were dried in an air oven, at 35 °C, for 1 week. The mass percent loss, measured regularly during the above time range, is quite large (Figure 5). Dry gels were properly cut, forced into glass tubes, added with distilled water, and sealed. Water uptake, inferred by the increase of the gel height with time, is noticeable.

SEM Microscopy. Measurements were performed at about 20 kV by a SEM-LEO1450VP unit, equipped with an INCA300 EDS microanalysis facility, as indicated elsewhere.[45,46] The gels were located on glass surfaces and sheared with polished mica, to make the film thickness uniform. The absence of optical anisotropic textures was controlled by polarizing microscopy, before transferring the samples into the SEM unit. The gels were dried at room temperature for 30 min. To minimize water loss

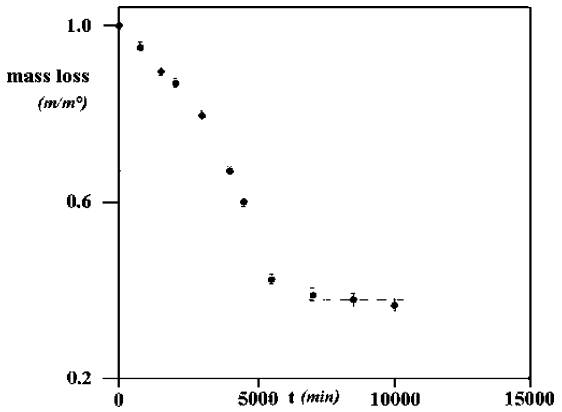

Figure 5. Dehydration of a gel containing 12.35 wt % BSA and 7.15 wt % NaTDC, put into an air oven at 35 °C, reported as normalized mass loss ($m/m°$) vs t, in minutes ($m°$ is the initial gel mass). The final product is transparent and glasslike. The dotted line indicates the long time limiting mass value.

and enhance conductivity, the gels were covered with gold by vapor sputtering. The size and shape of the textures observed are practically insensitive to the preparation procedures. Similar textures were obtained on dry (non-gold-covered) gels. A typical SEM texture of the dry gel phase is reported in Figure 6.

NMR Self-Diffusion. Pulsed gradient spin−echo methods (PGSE-NMR) were used. A Varian FT 80 spectrometer operating on ^{1}H nuclei and equipped with a Stelar pulsed magnetic field gradient unit was used to perform the measurements. The temperature was kept at 25.00 ± 0.02 °C by means of a VTC87 Stelar temperature controller.

The spin−echo attenuation obeys the equation[47]

$$I = I° \exp\left(\frac{-2\Delta}{T_2}\right) \exp\left[-(g\gamma\delta)^2 D^*\left(\Delta - \frac{\delta}{3}\right)\right] \qquad (1)$$

where γ is the gyromagnetic ratio of proton, D^* is the experimental self-diffusion coefficient of HDO, g is the strength of the applied gradient, T_2 is the proton relaxation time of HDO, and Δ and δ are the time parameters used in the pulse sequence. No stimulated echo methods were used, despite the high viscosity of the system. Details on PGSE sequences and data handling are given elsewhere.[48]

Signals relative to the protein or the surfactant are broad and could not be observed with due accuracy. That is why only data relative to HDO molecules are considered (Figure 7).

^{23}Na NMR Relaxation. The ^{23}Na NMR measurements were performed by a JEOL Eclipse 400 spectrometer (9.4 T) operating at 400 MHz for ^{1}H and 105.75 MHz for ^{23}Na and equipped with a JEOL NM-EVTS3 variable temperature unit, using 1 K complex data points for spectral widths of 600 Hz. The ^{23}Na longitudinal relaxation times, T_1, were determined by inversion recovery using 19 intervals, and the transverse relaxation times, T_2, were determined, using the same intervals as above, by means of Hahn echo. Some data are reported in Table 1. The double quantum filtered spectra were recorded at 30 °C using the pulse sequence reported in the literature.[49]

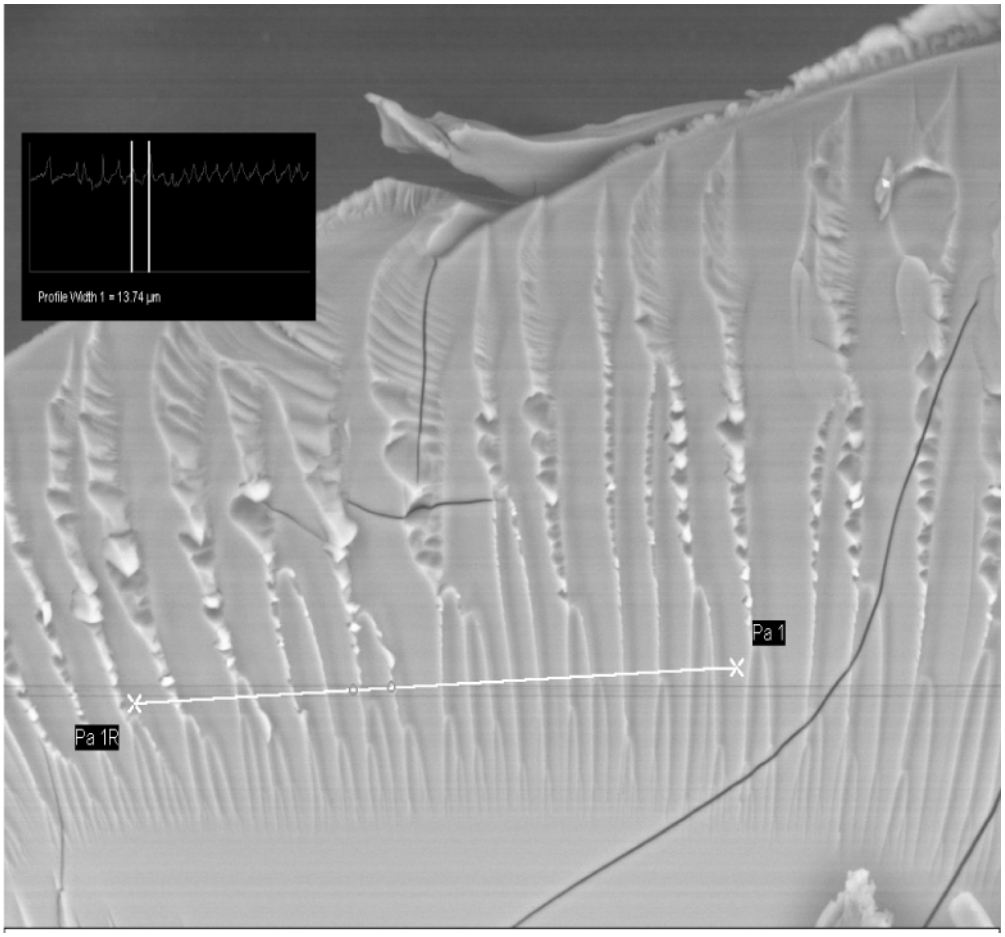

Figure 6. SEM textures observed on a dry gel, originally containing 10.00 wt % BSA and 5.00 wt % NaTDC. The gel was reduced to small pieces by an agate mortar and equilibrated at room temperature for 30 min before being covered with gold. The size of the bar on the left is 25 μm. The inset shows the repetition distances between fibrous textures.

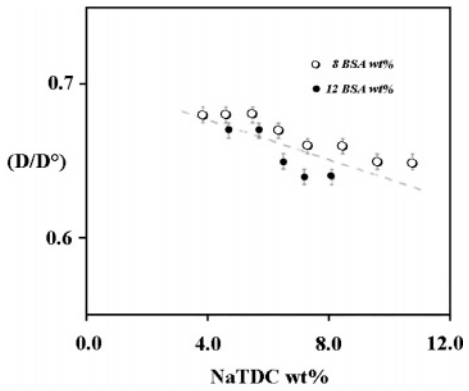

Figure 7. Water self-diffusion values, relative to HDO, at 25.0 °C vs bile salt content (in wt %) for selected water−BSA−NaTDC gels.

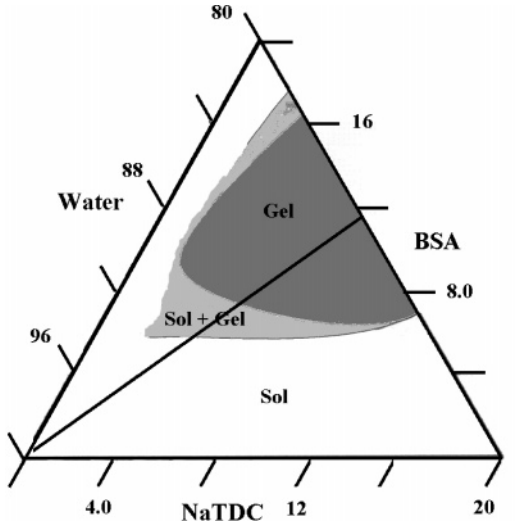

Figure 8. Partial phase diagram of the water−BSA−NaTDC system, at pH 6.4 and 25.0 °C. The full line dividing the gel phase into two parts is the charge neutralization one. The two-phase region is indicated in light gray color, and the gel, in dark gray.

Results

Partial Phase Diagrams. In Figures 8 and 9 are reported the partial phase diagrams of the system composed of water (or water−HCl), BSA, and NaTDC. The investigated region is limited to concentration regimes where the protein is soluble and no liquid crystalline phase, or two-phase system, is formed by the bile salt.[13,14] In such figures, data relative to spontaneous pH conditions (around 6.4), pH 5.0 and 3.0, respectively, are reported. pH affects strongly the precipitation and, to a much smaller extent, the width of the gel phase.

The phase behavior investigated in more detail refers to three different experimental conditions, that is, when (1) interactions between similarly charged objects take place (pH ≥ 6.4), (2) interactions between charged surfactants and uncharged protein occur (pH ≈ 5.0), and (3) BSA and bile salts are oppositely charged (pH close to 3.0).

The ones mentioned above are schematic representations of a more complex behavior.

At the isoelectric point of BSA, there is an equivalent number of positive and negative charges facing the outside of the protein surface and the occurrence of electrostatic interactions between positively charged groups of the protein and BS cannot be ruled out "a priori". In the following, we discuss separately the different phases which have been investigated.

Solution Region. Under spontaneous pH conditions, the occurrence of a wide solution phase, extending from the BS-rich side to the protein-rich side, is observed, as indicated in Figure 8. Most thermodynamic properties in the above region are similar to those observed in micelle forming systems in the presence of a polymer.[50] Addition of BSA is concomitant to a shift of cmc toward higher concentration. Such delay in forming free micelles is presumably related to a saturation of the protein binding sites by NaTDC.

The enthalpy and Gibbs energy associated with the transfer of NaTDC from water to water−BSA systems indicate the occurrence of significant interactions between the components, which are responsible for the overall system stability.[51] Obviously, the interactions depend on the BSA content in the mixture. The number of binding sites on the protein increases by lowering the pH of the medium. The pH, for instance, has a strong influence on the enthalpy of BS transfer from water to water−BSA mixtures.[52]

The ionic conductivity indicates the occurrence of a critical threshold required to get free micelles, which is slightly higher than that in H_2O. It must be noted also that the ionic conductivity values for NaTDC in the presence of BSA are significantly lower than those in neat water, as expected. The ionic conductivity data suggest that about 18−20 NaTDC molecules are required to saturate the protein binding sites when the pH is 6.4. This can be seen by examining Figure 2, which clearly indicates that the overall surfactant mobility increases once BSA saturation is completed.

The number of molecules interacting with the protein can be evaluated according to a mean spherical approximation model for the ionic conductivity of micelles, or supramolecular aggregates.[53] The model predicts the occurrence of as many forces as the ionic species in solution (BSA, micelles, TDC^-, and Na^+ ions). The relaxing contributions to conductivity depend on a first-order perturbation to the pair distribution function, $L_{j,i}$.

In that model, the diffusion modes relative to each ionic species influence each other according to

$$L_{j,i} = \left(\frac{e_i D^\circ_i - e_j D^\circ_j}{D^\circ_i + D^\circ_j}\right)(n_i e_i n_j e_j) \qquad (2)$$

where the subscripts refer to the different components, *e* and *n*

TABLE 1: ^{23}Na NMR Longitudinal, T_1, and Transverse, T_2, Relaxation Times in Aqueous NaBr and in Selected Gels, at Different Temperatures

θ (°C)	0.2 M NaBr $T_1/10^{-3}$ s	10.09 wt % BSA 5.16 wt % NaTDC $T_1/10^{-3}$ s	10.09 wt % BSA 5.16 wt % NaTDC $T_2/10^{-3}$ s	12.05 wt % BSA 5.97 wt % NaTDC $T_1/10^{-3}$ s	12.05 wt % BSA 5.97 wt % NaTDC $T_2/10^{-3}$ s
25.0	57.7	29.4	20.3	27.6	18.1
30.0	63.6	32.0	22.5	30.0	19.9
35.0	67.3	34.3	24.2	31.8	21.4
40.0	72.6	37.2	26.5	34.1	23.2
45.0	76.4	40.0	28.8	37.0	25.3
50.0		42.0	31.1	39.0	27.0

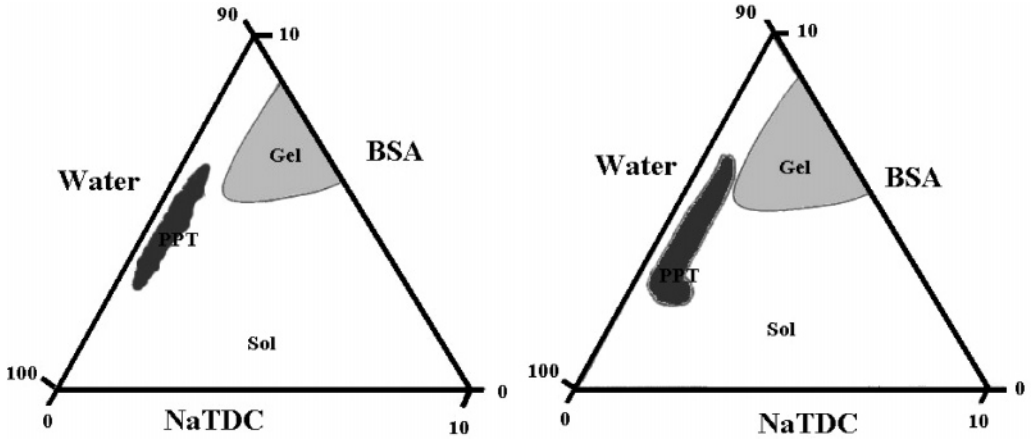

Figure 9. Partial phase diagrams of the (pseudosolvent)−BSA−NaTDC systems, at pH 5.0 (left) and 3.0 (right) and at 25.0 °C. The gel is indicated in light gray color, and the precipitate, in dark gray. The two-phase region gel + solution is not shown.

are the charge and number concentration, respectively, and the limiting self-diffusion coefficients, $D°$, are obtained from literature data.[54]

Thereafter, the ionic radii of the different species are introduced, to calculate the ionic conductivity. The data, corrected for the respective hydrodynamic contributions,[55] give a specific conductivity value, χ_{sp}, in the presence of different interionic forces, which can be expressed according to[53]

$$\chi_{sp} = \left[\frac{10e^2N_A}{k_BT}\right]\sum_{i=1}^{n} c_i D°_i z_i^2 \left[1 + \left(\frac{\delta v_{i,hydr}}{v_i}\right)\right]\left[1 + \left(\frac{\delta \kappa_{i,rel}}{\kappa_i}\right)\right] \quad (3)$$

where c_i is the concentration of each species, z_i is the valence, and $v_{i,hydr}$ and $\kappa_{i,rel}$ are the hydrodynamic velocity and the relaxing contributions, respectively. Other symbols have their usual meaning. χ_{sp} data are transformed into equivalent conductance values and iteratively compared with the experimental ones, up to convergence.

In a first approximation, the mobility of the protein−TDC_N adducts is assumed to be nearly the same as that of the free protein (N.B., the subscript N indicates the number of TDC^- ions interacting with BSA). Eventual corrections were made during the iterative procedure. In words, the observed decrease in ionic conductivity is essentially due to the partial charge neutralization of ionic groups on BSA by BS. Sodium binding onto BSA−TDC_N complexes is not accounted for. The above approximations are realistic when the sizes of the different species are taken into consideration (about 4.0 nm for BSA, 0.7 nm for TDC, and 0.11 nm for sodium ions). At the end of the iterative procedure, the size of the protein−surfactant complex was evaluated to be 4.3−4.5 nm. Once binding is completed, a slight, but regular increase in conductivity, due to small BS micelles and free ions, is observed. Despite the many approximations used in the above approach, the nice correlation between the number of binding sites and conductivity values is noteworthy. The latter method, in fact, gives a clear indication of the occurrence of protein saturation thresholds, centered around 18−20 BS molecules per protein. Micelle formation, conversely, occurs once the binding sites onto the protein have been saturated by surfactant ions.

Gel Phase. In the central portion of the phase diagram, a wide gel phase, surrounded by a two-phase region, is observed. Gels are highly viscous and do not easily flow under their own weight. They have the typical consistency of protein-based gels; that is, they are essentially plastic and resilient to touch.[56]

The gels almost reversibly shrink or swell (upon rehydration); nevertheless, they retain a nearly transparent appearance. Strongly dehydrated gels can be crashed into pieces; the gel, under such conditions, looks like a glassy solid. The physicochemical characterization of the gel phase was performed by combining sodium ion relaxation, water self-diffusion, rheology, and DSC, which are reported below.

Measurements of ^{23}Na NMR transverse relaxation times can be successfully exploited to gain information on soft materials such as biopolymers, gels, or biological tissues.[57,58] ^{23}Na nuclei possess a spin quantum number of $I = {}^3/_2$ and a quadrupole moment of 0.1089×10^{-28} m^2,[59] so that their relaxation is mainly due to a quadrupolar mechanism rooted in the fluctuations of the electric field gradient (EFG) at the nuclear site of the hydrated sodium ion, which, in concentrated surfactant or biopolymer solutions, have different origins and time scales.[60−62] When the slow motions are overwhelming, the signal is the sum of two Lorentzian lines. The former is related to the $[-{}^1/_2 \rightarrow +{}^1/_2]$ transition, and the latter, broader, to the $[-{}^3/_2 \rightarrow -{}^1/_2]$ and the $[+{}^1/_2 \rightarrow +{}^3/_2]$ ones. The presence of slow motions is manifested by the biexponential character of the relaxation curves[58] and by the possibility of observing signals in the spectra acquired with multiquantum filters (MQF).[63,64]

The ^{23}Na NMR transverse relaxation time measurements were carried out from 25.0 to 50 °C, on two gel samples at a water content higher than 80 wt %. For both samples considered, the curves of transverse relaxation are monoexponential and no signal could be detected in the double quantum filtered spectra, indicating that very slow motions do not provide the main contribution to sodium ion relaxation. The transverse relaxation rates ($R_2 = 1/T_2$) are higher than the longitudinal ones ($R_1 = 1/T_1$). Both R_2 and R_1 decrease upon increasing temperature, and their difference decreases (Table 1). The inequality of the two relaxation rates indicates that neither system is under extreme narrowing conditions. The activation energies relevant to R_2 dynamics are reported in Table 2.

Only the solvent self-diffusion could be determined with some accuracy in gel phases, because the very large signal width of both the protein and the bile salt does not allow an univocal assignment. The self-diffusion coefficients of NaTDC aqueous solutions have been widely investigated by some of us.[13] They decrease significantly with surfactant content, because of a significant growth in aggregate size. Addition of BSA further decreases the self-diffusion values of NaTDC, which are hardly determined by classical pulse sequences. Inherent values, thus, are subjected to a large uncertainty. As reported in Figure 7,

TABLE 2: Activation Energy from Sodium Transverse NMR Relaxation Time, in kJ mol^{-1}, of NaBr, of Gel 1 (10.09 wt % BSA, 5.16 wt % NaTDC), and Gel 2 (12.05 wt % BSA, 5.97 wt % NaTDC)[a]

system	E_{att} (kJ mol^{-1})	ΔE_{att} (kJ mol^{-1})
0.2 M NaBr	10.9	0.3
gel 1	13.6	0.4
gel 2	12.8	0.3

[a] Data were calculated by an Arrhenius T_2 data fit in the temperature range 25.0−50.0 °C. Errors on the activation energies are reported in column 3.

the water self-diffusion in the gels is only slightly dependent on composition. In words, the obstruction to water self-diffusion, which is reflected in the absolute self-diffusion values, does not change much with composition. Raw self-diffusion data may be of limited utility, if not properly linked with more information on the system properties. In the present case, they indicate that the system is water continuous and allow getting estimates on the amount of bound water molecules. Roughly 1 gram of the protein−surfactant complex adsorbs the same amount of water. More generally, self-diffusion supports information from sodium NMR relaxation methods.

At low T, the real and imaginary components of the viscoelastic spectrum, G' and G'', are constant in the whole stress range, whereas a marked dependence on σ is observed above 45.0 °C. At 20.0 °C, $G'' > G'$; the reverse behavior holds above 40 °C. Temperature ramp experiments, performed at $\sigma = 5.0$ Pa, 1 °C min^{-1}, and 1.0 Hz, checked the occurrence of thermal gelation thresholds (TGT)[65,66] (Figure 4). Above 70−80 °C, the protein denatures. G' and G'' values of PS gels containing denatured BSA are much different from those obtained by the above procedures (performed on heating) and are not reported.

It was not possible to get structural information on the gels. Thus, guesses on the reciprocal arrangement of BSA and NaTDC in such a phase rely on information available from small-angle X-ray scattering (SAXS) data relative to a structurally related protein−surfactant-based gel containing lysozyme and sodium dodecyl sulfate.[67] Therein, the reciprocal arrangement of protein and surfactant molecules results in the formation of a phase composed of structural units containing eight protein molecules each, and the corresponding number of surfactant species, forming rodlike aggregates. Assuming the same phase organization to be valid in the present case too, the approximate constancy of self-diffusion values in a wide composition range can be safely accounted for.

The rheological characterization of the gels was performed as a function of frequency and temperature, in a wide range of protein-to-surfactant ratios. Even though the whole area in Figure 8 is schematically considered a gel in the phase diagram, significant differences are observed from region to region in that phase. If the classical physical definition of gel is accounted for (i.e., a "true" gel is such when $G' > G''$),[42] then the width of the true gel region is lower than the one reported in Figure 8; it shrinks with an increase in temperature and almost regularly depends on the NaTDC/BSA mole ratio. This behavior is particularly evident in the dependence of the thermal gelation threshold, T_G, on the aforementioned ratio (Figure 10). Accordingly, there is a slight, but significant increase of T_G values with the amount of bile acid salt, with the amount of protein in the mixture playing a minor role in such transitions.

According to the definition of a true gel, originally proposed for polymer-based gels,[68] the region where $G' \leq G''$ is to be considered a viscous solution, even though the samples do not flow after being kept under gravity conditions for days or weeks.

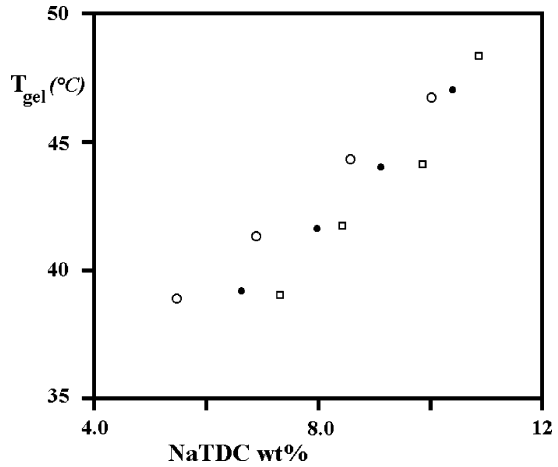

Figure 10. Dependence of the thermal gelation threshold, T_G (°C), on the NaTDC/BSA mole ratio, for samples containing 10.16 (○), 12.05 (●), and 14.11 (□) wt % BSA. T_G values were obtained by plotting G' and G'' values versus T, when the shear stress, σ, is 5 Pa, and considering them as the intersection point of the two curves. Errors are to ±1.0 °C.

To evaluate the dependence of the viscoelastic properties (both the amplitudes and frequencies) on temperature and composition, data were plotted as a function of the following generalized equations[42]

$$G'_{\sigma}(\omega) = \sum_{i=1} G_i^{\circ}\left[\frac{(\omega\tau_i)^2}{1+(\omega\tau_i)^2}\right] \tag{4A}$$

$$G''_{\sigma}(\omega) = \sum_{i=1} G_i^{\circ}\left[\frac{\omega\tau_i}{1+(\omega\tau_i)^2}\right] \tag{4B}$$

ω is the applied frequency, in hertz, τ_i is the relaxation time associated with the ith relaxation process, and G_i° is the corresponding amplitude. Thus, the elastic, G', and viscous, G'', contributions to the overall spectrum could be evaluated. All data were measured at a fixed shear stress, $\sigma = 5$ Pa. Before proceeding further, estimates on the occurrence of one or more viscoelastic relaxation processes were inferred by plotting the function[69]

$$\tau = \left(\frac{1}{\omega}\right)\left(\frac{G'}{G''}\right) \tag{5}$$

which is linear only when a single relaxation process occurs. Departures from the linear behavior indicate the presence of two or more relaxation processes, with changes in slope at the corresponding frequencies. Generally, three well separated relaxation processes fit the data with an appreciable accuracy, as indicated in Figure 11. This behavior holds above the thermal gelation threshold, and the fits refer to that regime. The situation is quite different below T_G, where a Maxwell-like (continuous) distribution of relaxation times occurs.[70]

For temperatures above and below that value, the generalized dynamic viscosity, $\eta_{\sigma}^*(\omega)$, can be written as[42,71]

$$\eta_{\sigma}^*(\omega) = \left(\frac{1}{\omega}\right)\sqrt{[G'_{\sigma}(\omega)]^2 + [G''_{\sigma}(\omega)]^2} \tag{6}$$

where the meaning of symbols is as before.

It is remarkable to note that, in the limits of existence of the true gel, the relaxation frequencies of the different dynamic

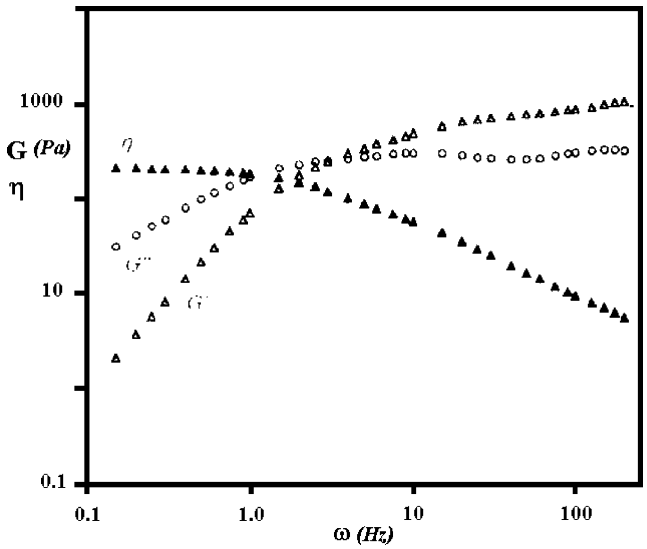

Figure 11. Viscoelastic relaxation spectrum for a sample containing 10.24 wt % BSA with 6.7 wt % NaTDC, at 25 °C. The G' (△), G'' (○), and η (▲) values (in Pa) are reported versus log ω (in Hz).

processes depend quite regularly on both composition and temperature, as indicated in Table 3.

Further relevant aspects of the gel phase come out from the analysis of DSC data (Table 4). The T_G values inferred from the presence of small endothermic peaks in the calorimetric data are in fairly good agreement with those inferred from rheological findings, as formerly shown by some of us on a structurally related protein−surfactant-based gel.[69] Relevant too is the upward shift of the BSA thermal denaturation in the gel, 8−10° high. In words, the thermal stability of the protein in such a gel is higher than that in solution, even though the heat effect associated with the process is roughly the same as that in bulk water.[26]

Precipitate Region. At pH 5.0 and, to a much larger extent, at pH 3.0, precipitation of protein−surfactant complex(es) takes place. The precipitation rate depends on protein and surfactant concentration, mole (charge) ratio, pH, solution viscosity, and temperature. In some instances, the precipitates do form at the interface between two stratified liquids and look like persistent whitish membranes (Figure 12) stable under moderate shear. In others, platelets or small crystals are observed. The latter two forms dominate at low pH values. The structure of the crystals, presumably, reflects the conformation of the protein under such conditions. In fact, BSA forms anisotropic particles

TABLE 3: Slow, Intermediate, and Fast Viscoelastic Relaxation Times, τ_1, τ_2, and τ_3, Respectively (in ms), for True Gels, at Different Temperatures[a]

	12.4 wt % BSA + 6.7 wt % NaTDc			14.3 wt % BSA + 6.9 wt % NaTDC		
temperature (°C)	τ_1 (ms)	τ_2 (ms)	τ_3 (ms)	τ_1 (ms)	τ_2 (ms)	τ_3 (ms)
25.0	530	83	5.5	620	115	9.4
35.0	430	75	5.0	500	103	8.5
40.0	365	71	4.6	430	91	8.0
45.0	310	67	4.1	370	80	7.3
50.0	286	66	3.6	315	72	6.7
55.0	250	70		290	65	60
65.0	154	64	2.8	236	59	5.2

[a] Errors on τ_i values are lower than 3%; those relative to τ_3 are about 6−8%. The measuring temperature (in °C) is reported in the leftmost column.

TABLE 4: BSA Denaturation Temperature, Θ_{den}, in °C, and the Related Enthalpy, ΔH_{den}, in J g^{-1}, for Selected Gel Samples, as Inferred by DSC Findings[a]

medium	Θ_{den} (°C)	ΔH_{den} (J g^{-1})
water	62.0 (±0.3)[b]	1.75 (±0.03)[b]
10.0 wt % BSA + 6.0 wt % NaTDC	71.3 (±0.4)	1.68 (±0.03)
11.1 wt % BSA + 6.0 wt % NaTDC	79.2 (±0.4)	1.74 (±0.03)
12.0 wt % BSA + 6.0 wt % NaTDC	80.3 (±0.4)	1.73 (±0.02)
14.0 wt % BSA + 6.1 wt % NaTDC	74.7 (±0.3)	1.72 (±0.03)
14.0 wt % BSA + 8.0 wt % NaTDC	81.4 (±0.3)	1.81 (±0.04)

[a] The composition of the individual gel samples, in wt %, is reported on the left-hand side column. Measurements were performed at a scan rate of 1.0 °C min^{-1}. [b] From ref 26.

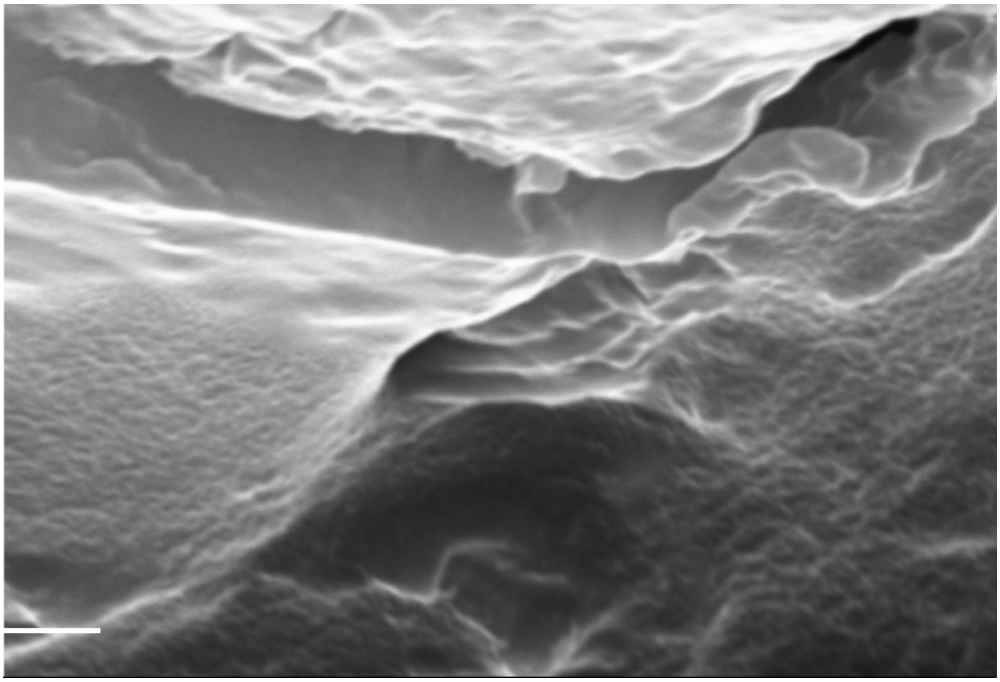

Figure 12. SEM image of the whitish mucous solid stratified at the liquid−liquid interface after addition of 1.0 mL of 0.01 M HCl to 1.0 mL of a solution containing 1.35 wt % BSA and 1.8 wt % NaTDC. The bar is 1 μm long.

close to pH 5.0 and elongated fibers at pH 3.0.[72] This may have consequences on the crystalline form of the BSA−$(NaTDC)_N$ complexes and precipitates.

A relevant aspect which can be fortuitous, but requires careful attention, is that the location of the precipitate in the (pseudo)-phase diagrams divides the concentration regime pertinent to entero-hepatic from that peculiar to cholecystic bile.[73]

Discussion

Many aspects depicted here need to be considered in more detail: the effect of pH, for instance, is important in many phenomena related to the entero-hepatic circulation. The same holds for the formation of poorly soluble protein−surfactant precipitates. Some of the above aspects have been clarified in recent articles.[74,75] That is why, in the following, attention is mainly focused to the behavior observed in gel phases.

The reasons for so much interest in PSS are of fundamental significance, because they may help the understanding of the behavior of proteins in real biological matrixes (often having gel-like consistency). Even practical applications, however, may be important.[23]

The gels formed in PSS have been recently investigated by Khan et al.,[76−78] Almgren,[79] and some of us.[30,80] Peculiar is the location of the PS gels in the phase diagram, usually between the precipitate and the micellar solution. The gels are thermodynamically stable and strongly viscous. Information available up to now spans from NMR relaxation[81] to SAXS.[67] There are, however, many aspects which deserve more consideration. Indeed, many aspects pertinent to the gel nature may be inferred by combining thermodynamic analysis, rheological methods (which give information on their mechanical stability), and structural and spectroscopic methods, to define in more detail which forces are responsible for their stability. Even transport properties, self-diffusion, for instance, can be relevant for the above purposes.

NMR. The most adequate model for systems made up of surfactants and/or polymers does not deal with a single viscous homogeneous medium but is the two-site approach in which one distinguishes sodium in bulk water from sodium associated with the aggregates.[82] The relaxation rates are thus expressed in terms of exchange-averaged spectral density functions, that are the result of the averaging over the various sites visited by the sodium cation. The spectral density functions summarize the motional features that determine sodium relaxation.

$$R_{1[-1/2\rightarrow+1/2]} = 2J(\omega_0)$$

$$R_{1[-3/2\rightarrow-1/2]} = R_{1[+1/2\rightarrow+3/2]} = 2J(2\omega_0)$$

$$R_{2[-1/2\rightarrow+1/2]} = J(\omega_0) + J(2\omega_0)$$

$$R_{2[-3/2\rightarrow-1/2]} = R_{2[+1/2\rightarrow+3/2]} = J(0) + J(\omega_0) \qquad (7)$$

where ω_0 is the Larmor frequency and the spectral density function, J, includes the quadrupolar coupling constant.[83] R_1 and R_2 are the relaxation rates relevant to sodium longitudinal and transverse magnetization, respectively. In extreme narrowing, $J(0) = J(\omega_0) = J(2\omega_0)$, so that $R_{1[-1/2\rightarrow+1/2]} = R_{1[-3/2\rightarrow-1/2]} = R_{1[+1/2\rightarrow+3/2]} = R_1$ and $R_{2[-1/2\rightarrow+1/2]} = R_{2[-3/2\rightarrow-1/2]} = R_{2[+1/2\rightarrow+3/2]} = R_2$ and, furthermore, $R_1 = R_2$. The exit from extreme narrowing is signaled by R_2 becoming larger than R_1.

The two-step model[84−86] has been extensively employed in the interpretation of counterion relaxation parameters.[87] It expresses the spectral density function as the sum of two terms, that correspond to two uncorrelated motions occurring on widely different time scales.

$$J(\omega) = (1 - S^2)J_f(\omega) + S^2J_s(\omega) \qquad (8)$$

The former term, J_f, is related to hydration sphere dynamics fast for the ions both in bulk and in association with the aggregates and the consequent modulation of the EFG at the sodium nucleus, with a correlation time below 1 ps.[62,88] However, owing to the presence of the aggregates, the fast motions may fail to average completely out the EFG at sodium. The latter term, J_s, arises from the modulation of the residual EFG by motions occurring on a much slower time scale, on the order of nanoseconds, that is, by diffusion about the aggregate. The order parameter S^2 accounts for the amount of EFG not averaged by fast motions.

In Table 1 are reported the R_1 and R_2 values at various temperatures for the two gel samples examined, together with the R_1 data for a 0.2 M NaBr aqueous solution for reference purposes. The smooth trend of relaxation rates does not suggest the occurrence of phase transitions. For the NaBr aqueous solution, extreme narrowing holds and therefore $R_1 = R_2$.

For the two gel samples, sodium is outside extreme narrowing, since R_1 and R_2 are different, but not much, since transverse relaxation is not biexponential and no signal appeared in the DQF spectra. Therefore, the slow motion should have a τ_C value close to the reciprocal of the Larmor frequency. For $\nu_0 = 105.75$ MHz, $1/\omega_0 = 1.5$ ns. Such a value is on the order of magnitude of those (about 1−10 ns) determined from dielectric measurements for water molecules in the hydration layers of proteins.[89] A value of 4 ns was obtained from the relaxation parameters at a magnetic field of 1.9 T for BSA solutions with NaCl, in the concentration range 1.68−6.7%.[84] BSA solutions (20 and 30%), also in the presence of added NaCl, gave signals in MQF experiments,[90] at a magnetic field identical to that of our spectrometer, that is, 9.4 T. Furthermore, a value of 2.6 ns, obtained from MQF ^{23}Na line shapes, at 9.4 T, is reported for 40% aqueous BSA in 1 M NaCl.[63] It is worth mentioning that the occurrence and strengthening of ^{23}Na signals in MQF experiments from BSA solutions, that is, the presence of slow motions, is favored by an increased protein concentration and depends also on its tertiary structure that may be affected by the presence of simple electrolytes, such as NaCl or KCl.[91]

The lack of very slow motions for the sodium solvation sphere rules out a tight association of metal ion with the large TDC−BSA aggregates, that is probably hindered in the present gels by the interactions between TDC^- and BSA (electrostatic attraction between the bile salt anion and positively charged groups of the protein, hydrogen bonds, and hydrophobic interactions).

The activation energy for the dynamic processes is also a good probe to test whether, and to what extent, motion in PS-based gels is hindered compared to neat water. According to the data in Table 2, the activation energy of the motions responsible for T_2 NMR relaxation times is slightly higher compared to the case of bulk water, as if the motion were moderately hindered. The effect of composition on E_{att} is moderate. This is in fairly good agreement with what was observed in self-diffusion findings, which unequivocally indicate that water motion in such matrixes is practically insensitive to composition. Hence, the mobility of water and ions in such gels is not much different from that in aqueous solutions, even if the dynamic parameters indicate a slightly higher barrier to their motion. This could be a consequence of the reciprocal arrange-

ment of albumin and bile salts to form the gels and of the subsequent preferred location of the ions in such matrixes.

Rheology. As to the rheological behavior of the gels, the following information can be obtained from experiments. Above T_G, the storage modulus of the gels, G', becomes progressively higher with increasing temperature, where the opposite holds for the viscous component, G''. Above that temperature threshold, physical bonds between particles constituting the gel skeleton are strong, whatever the particles are. As formerly indicated, the reciprocal arrangement is possible in the gel of protein and surfactant molecules forming complexes or aggregates of some sort. The significantly high G' values imply a high number density of bonds between particles. In addition, high G' values indicate that protein−surfactant complexes in the gel are held together by relatively strong interactions. They form extended isotropic networks composed by the interconnection of such particles. The true gel domain is only part of the gel region in Figures 8 and 9. There, an essentially elastic material characterized by a three-dimensional isotropic network dominates (N.B., the gels are optically isotropic).

The dynamic response of the gels to shear stresses deserves some attention. As mentioned above, there is a remarkable variety of relaxation processes, generally a fast one, an intermediate one, and a slow one. The links between different relaxation times and the dependence of such dynamic quantities on composition, phase structure, and/or temperature may help the acquisition of information on the hierarchy of forces controlling them.

Fitting of rheological data is strongly model dependent, and the relaxation processes of real systems such as gels may have a continuous distribution or may be discrete. In the following, efforts shall be made to remark the differences between true and other gel phases. In the latter cases, a continuous distribution of relaxation processes can be accounted for and a Maxwell-like distribution function fits the data with an appreciably good accuracy. In the former, conversely, it results possible to assign univocally some major components to the viscoelastic spectrum. The differences between the rheological behavior of true and other gels shall be discussed in more detail below.

Recently, Coppola et al. proposed a hypothesis for the frequency dependence of viscoelastic relaxation processes in organized solutions.[92] Transforming frequency dependent, $G(\omega)$, into time dependent, $G(t)$, fits allows, in principle, the drawbacks inherent to fitting procedures to be overcome. Their approach, based on the use of inverse Laplace transforms, allowed them to distinguish among different relaxation rates and relaxation time distributions in the overall viscoelastic spectrum and could help the improvement of the fitting procedure. Perhaps the validity of fits based on continuous distributions is not always rational or physically consistent. It must be recalled, also, that operational approaches based on discrete relaxation modes are easy to handle.

In true gels, a discrete model shall be used to ascertain whether, and to what extent, it is possible to control the viscoelastic behavior by composition. An example of a fitting procedure in such a phase is reported in Figure 11. There, the occurrence of three main modes in the overall viscoelastic spectrum is evident. It is remarkable, on these grounds, to find links between composition and fitted relaxation times, or amplitudes. The former quantities, in particular, seem to be related to composition and mole ratios between the components (Figure 13). The results indicate that, at fixed BSA content, the slow relaxation times (tentatively ascribed to the interactions between adjacent protein−surfactant complexes in the gel)

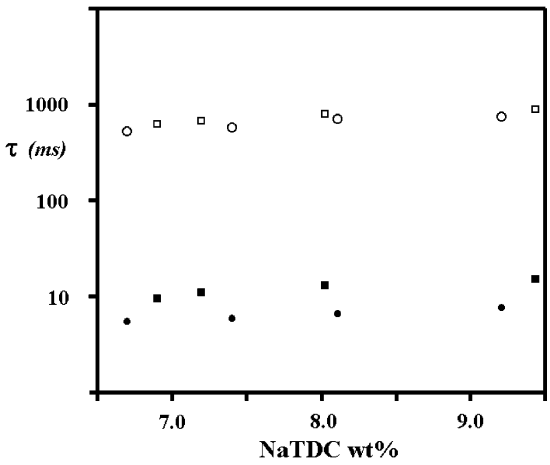

Figure 13. Semilogarithmic plot of the dependence of the slow (● or ■) and fast (○ or □) relaxation time, τ (in ms), on wt % NaTDC in true gels containing 12.05 (circles) and 14.11 (squares) wt % BSA, at 35.0 °C.

slightly increase with BS content. Such a behavior is presumably related to the number of links between different complexes in the gel, provided no morphological changes occur. In this context, the data satisfy the structural model developed by Stenstam,[67] supposing the arrangement of many protein−surfactant clusters in interconnected rodlike aggregates.

According to the data in Figures 11 and 13, the similarity of the present gels to polymeric melts as well as to dilute suspensions of anisometric particles must be pointed out. This is particularly evident in the shape of $G''(\omega)$ curves. The presence of a shallow minimum therein is typical of concentrated polymeric liquids and/or rodlike particles in solution, for instance.[42,71] These facts can be exploited for a tentative structural characterization of the PS gels. Keeping in mind the limits inherent to the experimental methods (giving indirect structural proofs) and considering the gels as relatively dilute systems, the possible rodlike arrangement of particles, proposed according to small-angle neutron scattering (SANS) data[67] comes out from the analysis of $G''(\omega)$ data. Such a hypothesis, however, is tentative and needs to be supported by cogent structural investigation.

Conclusions

The purpose of this work was to get information on aqueous solutions, precipitates, and gels formed by mixing a globular protein, bovine serum albumin, and a bile salt. The major consequences arising from the present investigation deal with the rich polymorphic behavior of the resulting ternary system. In particular, a gel phase was determined and characterized. The occurrence of a precipitate region, whose width increases by lowering the pH of the medium, was observed.[93] This can be a direct consequence of the increased number of binding sites and, accordingly, of the more compact arrangement, as well as of the number of charged groups onto the protein available to interact with BS. Slight changes in the number of links modify the apparent precipitate morphology.

Investigations were focused to characterize the gel phase, and a lot of experimental work was collected for that purpose. NMR and rheology, in particular, offer the possibility to draw some preliminary conclusions and to address future work along this line. The gel phase can be tentatively divided into two regions, one characterized by a typical gel-like behavior, that is, $G' > G''$. The region of existence of the true gel is modulated by BS/BSA mole ratios and decreases with increasing temperature.

The reciprocal arrangement of protein−BS clusters in the gel is responsible for their stiffness and complex rheological behavior and at the same time accounts for the nearly constant self-diffusion values of water and for the moderate activation energies to ion motion, inferred by ^{23}Na ion relaxation.

Finally, there is a remarkable stabilizing effect of the gel structure on the thermal stability of the protein. The thermal denaturation of BSA in such matrixes takes place at temperatures 8−10 °C higher than those in the bulk. This behavior is presumably due to the formation of protein surfactant clusters, held together in the gel by the combination of electrostatic and hydrophobic contributions.

Acknowledgment. We would like A. Capalbi, L. Galantini, E. Giglio, and N. V. Pavel, Department of Chemistry at La Sapienza (Rome), L. Coppola and G. A. Ranieri, Department of Chemistry at Unical (Arcavacata di Rende, CS), and A. L. Segre, Inst. Chem. Methodol. (CNR, Montelibretti, RM) for many stimulating discussions during the manuscript preparation. *MIUR*, the Ministry of Education, University and Research, supported this work through a *COFIN* project on polymer−surfactant systems, Grant No. 2002037154-001 (for the years 2002−2004). This research line was performed under the auspices of the European Community, by a *COST D-15 Action* Project on Interfacial Chemistry and Catalysis, 2000−2004.

References and Notes

(1) Carey, M. C.; Small, D. M. *Arch. Intern. Med*. **1972**, *130*, 506. Small, D. M.; Dowling, R. H.; Redinger, R. N. *Arch. Intern. Med*. **1972**, *130*, 552.

(2) Hofmann, A. F.; Roda, A. *J. Lipid Res*. **1984**, *25*, 1477.

(3) Hjelm, R. P.; Thiyagarajan, P.; Schteingart, C.; Hofmann, A. F.; Alkan-Onyuksel, H.; Ton-Nu, H.-T. *Falk Symp*. **1995**, *80*, 41.

(4) Hofmann, A. F.; Mysels, K. J. *Colloids Surf*. **1988**, *30*, 145.

(5) Hjelm, R. P.; Schteingart, C.; Hofmann, A. F.; Sivia, D. S. *J. Phys. Chem*. **1995**, *99*, 16395. Hjelm, R. P.; Schteingart, C. D.; Hofmann, A. F.; Thiyagarajan, P.; Manuel, L., Jr. *J. Phys. Chem. B* **2000**, *104*, 197.

(6) Carey, M. C.; Small, D. M. *J. Colloid Interface Sci*. **1969**, *31*, 382.

(7) Jones, C. A.; Hofmann, A. F.; Mysels, K. J.; Roda, A. *J. Colloid Interface Sci*. **1986**, *114*, 452. Hofmann, A. F.; Mysels, K. J. *J. Lipid Res*. **1992**, *33*, 617.

(8) Sesta, B.; La Mesa, C.; Bonincontro, A.; Cametti, C.; Di Biasio, A. *Ber. Bunsen-Ges. Phys. Chem*. **1981**, *85*, 798. Sesta, B.; La Mesa, C.; Bonincontro, A.; Cametti, C.; Di Biasio, A. *Ber. Bunsen-Ges. Phys. Chem*. **1982**, *86*, 664.

(9) La Mesa, C. *Recent Res. Dev. Surf. Colloids* **2004**, *1*, 97.

(10) Campanelli, A. R.; Candeloro De Santis, S.; Galantini, L.; Giglio, E.; Scaramuzza, L. *J. Inclusion Phenom. Mol. Recognit. Chem*. **1991**, *10*, 367.

(11) Campanelli, A. R.; Candeloro de Sanctis, S.; Chiessi, E.; D'Alagni, M.; Giglio, E.; Scaramuzza, L. *J. Phys. Chem*. **1989**, *93*, 1536.

(12) Mukerjee, P.; Mysels, K. J. *Critical Micellar Concentration of Aqueous Surfactant Systems*; NSR-DS, NBS: Washington, DC, 1971.

(13) Edlund, H.; Khan, A.; La Mesa, C. *Langmuir* **1998**, *14*, 3691. Marques, E. F.; Edlund, H.; La Mesa, C.; Khan, A. *Langmuir* **2000**, *16*, 5178.

(14) Amenitsch, H.; Edlund, H.; Marques, E. F.; Khan, A.; La Mesa, C. *Colloids Surf., A* **2003**, *213*, 79.

(15) Campanelli, A. R.; Candeloro de Sanctis, S.; Giglio, E.; Pavel, N. V.; Quagliata, C. *J. Inclusion Phenom. Mol. Recognit. Chem*. **1989**, *7*, 391. Galantini, L.; Giglio, E.; La Mesa, C.; Pavel, N. V.; Punzo, F. *Langmuir* **2002**, *18*, 2812.

(16) Tiddy, G. J. T. *Phys. Rep*. **1980**, *57*, 1. Larsson, K. *Lipids−Molecular Organisation, Physical Functions and Technical Applications*; The Oily Press: Dundee, Scotland, 1994; Chapter II, p 47.

(17) Schurtenberger, P.; Mazer, N. A.; Kaenzig, W. *Hepatology* **1984**, *4*, 143S. Mazer, N. A.; Schurtenberger, P.; Carey, M. C.; Preisig, R.; Weigand, K.; Kaenzig, W. *Biochemistry* **1984**, *23*, 1994. Schurtenberger, P.; Mazer, N. A.; Kaenzig, W. *J. Phys. Chem*. **1985**, *89*, 1042.

(18) Small, D. M.; Bourges, M.; Dervichian, D. G. *Nature* **1966**, *211*, 816. Small, D. M.; Bourges, M.; Dervichian, D. G. *Biochim. Biophys. Acta* **1966**, *125*, 563. Bourges, M.; Small, D. M.; Dervichian, D. G. *Biochim. Biophys. Acta* **1967**, *144*, 189. Ulmius, J.; Lindblom, G.; Wennerström, H.; Johansson, L. B. A.; Fontell, K.; Söderman, O.; Arvidson, G. *Biochemistry* **1982**, *21*, 1553.

(19) Roda, A.; Cappelleri, G.; Aldini, R.; Roda, E.; Barbara, L. *J. Lipid Res*. **1982**, *23*, 490. Scagnolari, F.; Roda, A.; Fini, A.; Grigolo, B. *Biochim. Biophys. Acta* **1984**, *791*, 274.

(20) Benz, R. W.; Tobias, D. J. *Abstracts of Papers, 229th ACS National Meeting*, San Diego, CA, March 13−17, 2005, COLL-294.

(21) Saitoh, T.; Fukuda, T.; Tani, H.; Kamidate, T.; Watanabe, H. *Anal. Sci*. **1996**, *12*, 569.

(22) Cabral, D. J.; Hamilton, J. A.; Small, D. M. *J. Lipid Res*. **1986**, *27*, 334. Smidkova, M.; Spundova, M.; Marecek, Z.; Entlicher, G. *Fundam. Clin. Pharmacol*. **2003**, *17*, 331.

(23) Goddard, E. D. In *Interactions of Surfactants with Polymers and Proteins*; Goddard, E. D., Ananthapadmanabhan, K. P., Eds.; CRC Press: Boca Raton, FL, 1993; p 395.

(24) Roda, A.; Hofmann, A. F.; Mysels, K. J. *J. Biol. Chem*. **1983**, *258*, 6362.

(25) Waldmann, T. A. In *Albumin: Structure, Function and Uses*; Rosenoer, V. M., Oratz, M., Rothschild, M. A., Eds.; Pergamon Press: Oxford, U.K., 1977; p 255.

(26) Boye, J. J.; Inteaz, A.; Ismail, A. A. *J. Agric. Food Chem*. **1996**, *44*, 996.

(27) Luner, P. E.; Vander, K. D. *J. Pharm. Sci*. **2001**, *90*, 348.

(28) Nagadome, S.; Oda, H.; Hirata, Y.; Igimi, H.; Yamauchi, A.; Sasaki, Y.; Sugihara, G. *Colloid Polym. Sci*. **1995**, *273*, 701.

(29) Schurtenberger, P.; Mazer, N.; Waldvogel, S.; Kaenzig, W. *Biochim. Biophys. Acta* **1984**, *775*, 111.

(30) Palacios, A. C.; Sarnthein-Graf, C.; La Mesa, C. *Colloids Surf., A* **2003**, *228*, 25.

(31) Hirst, L. S.; Pynn, R.; Bruisma, R. F.; Safinya, C. R. *J. Chem. Phys*. **2005**, *123*, 104902.

(32) Monkos, K. *Biochim. Biophys. Acta* **2004**, *1700*, 27.

(33) Singh, M.; Chand, H.; Gupta, K. C. *Chem. Biodiversity* **2005**, *2*, 809.

(34) Ryan, M. T.; Chopra, R. K. *Biochim. Biophys. Acta* **1976**, *427*, 337.

(35) Lewis, S. D.; Misra, D. C.; Shafer, J. A. *Biochemistry* **1980**, *19*, 6129. Taboada, P.; Gutierrez-Pichel, M.; Barbosa, S.; Mosquera, V. *Phys. Chem. Chem. Phys*. **2004**, *6*, 5203.

(36) Sesta, B.; D'Aprano, A.; Maddalena, G.; Proietti, N. *Langmuir* **1995**, *11*, 2860.

(37) Saikia, P. M.; Kalita, A.; Gohain, B.; Sarma, S.; Dutta, R. K. *Colloids Surf., A* **2003**, *216*, 21.

(38) Angelakou, A.; Valsami, G.; Macheras, P.; Koupparis, M. *Eur. J. Pharm. Sci*. **1999**, *9*, 123.

(39) Iovino, A. M.S. Thesis, La Sapienza, Rome, 2001.

(40) Roversi, M. M.S. Thesis, La Sapienza, Rome, 2004.

(41) Gente, G.; Iovino, A.; La Mesa, C. *J. Colloid Interface Sci*. **2004**, *274*, 458.

(42) Macosko, C. W. *Rheology Principles, Measurements and Applications*; VCH: New York, 1993; Chapter III, p 109.

(43) Bonicelli, M. G.; Ceccaroni, G. F.; La Mesa, C. *Colloid Polym. Sci*. **1998**, *276*, 109.

(44) La Mesa, C.; Coppola, L.; Ranieri, G. A.; Terenzi, M.; Chidichimo, G. *Langmuir* **1992**, *8*, 2616.

(45) Barbetta, A.; Cameron, N. R. *Macromolecules* **2004**, *37*, 3202.

(46) Michiotti, P.; La Mesa, C.; Bonicelli, M. G.; Ceccaroni, G. F.; Ferragina, C.; Cifarelli, P. *Colloid Polym. Sci*. **2003**, *281*, 431.

(47) Stejskal, E. O.; Tanner, J. E. *J. Chem. Phys*. **1965**, *42*, 288.

(48) Vergara, A.; Paduano, L.; D'Errico, G.; Sartorio, R. *Phys. Chem. Chem. Phys*. **1999**, *1*, 4875.

(49) Kemp-Harper, R.; Brown, S. P.; Colan H. E.; Styles, P.; Wimperis, S. *Prog. Nucl. Magn. Reson. Spectrosc*. **1997**, *30*, 157.

(50) La Mesa, C. *J. Colloid Interface Sci*. **2005**, *286*, 148.

(51) Palacios, A. C.; Antonelli, M. L.; La Mesa, C. *Thermochim. Acta* **2004**, *418*, 69.

(52) Antonelli, M. L.; Capalbi, A.; Gente, G.; Palacios, A. C.; Sallustio, S.; La Mesa, C. *Colloids Surf., A* **2004**, *246*, 127.

(53) Turq, P.; Blum, L.; Bernard, O.; Kunz, W. *J. Phys. Chem*. **1995**, *99*, 822. Durand-Vidal, S.; Turq, P.; Bernard, O.; Treiner, C. *J. Phys. Chem. B* **1997**, *101*, 1713.

(54) Stilbs, P. *Prog. Nucl. Magn. Reson. Spectrosc*. **1987**, *19*, 1 and references therein.

(55) Bernard, O.; Turq, P.; Blum, L. *J. Phys. Chem*. **1991**, *95*, 9508.

(56) Waynewright, F. W. In *The Science and Technology of Gelatin*; Ward, A. G., Court, A., Eds.; Acad. Press: New York, 1977; p 507.

(57) Buist, R. J.; Deslauriers, R.; Saunders: J. K.; Mainwood, G. W. *Can. J. Physiol. Pharmacol*. **1991**, *69*, 1663.

(58) Woessner, D. E. *Concepts Magn. Reson*. **2001**, *13*, 294.

(59) *CRC Handbook of Chemistry and Physics*, 75th ed.; Lide, D. R., Ed.; CRC Press: Boca Raton, FL, 1994.

(60) Eliav, U.; Shinar, H.; Navon, G. *J. Magn. Reson*. **1992**, *98*, 223.

(61) Furo, I.; Halle, B.; Quist, P. O.; Wong, T. C. *J. Phys. Chem*. **1990**, *94*, 2600. Halle, B. *NATO Sci. Ser., Ser. A* **1999**, *305*, 233.

(62) Cesare Marincola, F.; Denisov, V.; Halle, B. *J. Am. Chem. Soc*. **2004**, *126*, 6739.
(63) Chung, C.-W.; Wimperis, S. *J. Magn. Reson*. **1990**, *88*, 440.
(64) Jaccard, G.; Wimperis, S.; Bodenhausen, G. *J. Chem. Phys*. **1986**, *85*, 6282.
(65) Cellesi, F.; Weber, W.; Fussenegger, M.; Hubbell, J. A.; Tirelli, N. *Biotechnol. Bioeng*. **2004**, *88*, 740.
(66) Seo, K. S.; Kim, M. S.; Khang, G.; Cho, S. H. Lee, H. B. *Polym. Prepr*. **2005**, *46*, 820.
(67) Stenstam, A.; Montalvo, G.; Grillo, I.; Gradzielski, M. *J. Phys. Chem. B* **2003**, *107*, 12331.
(68) Cordobes, F.; Partal, P.; Guerrero, A. *Rheol. Acta* **2004**, *43*, 184.
(69) Roversi, M.; La Mesa, C. *J. Colloid Interface Sci*. **2005**, *284*, 470.
(70) D'Arrigo, G.; Sesta, B.; La Mesa, C. *J. Chem. Phys*. **1980**, *73*, 4562. D'Arrigo, G.; La Mesa, C. *Phys. Rev. A* **1981**, *24*, 2187.
(71) Ferry, J. D. *Viscoelastic Properties of Polymers*; Wiley: New York, 1980.
(72) Nakamura, K.; Era, S.; Ozaki, Y.; Sogami, M.; Hayashi, T.; Muratami, M. *FEBS Lett*. **1997**, *417*, 375. Ferre, M. L.; Duchowicz, R.; Carrasco, B.; Garcia de la Torre, J.; Acuna, A. U. *Biophys. J*. **2001**, *80*, 2422.
(73) Mazer, N. A.; Carey, M. C. *J. Lipid Res*. **1984**, *25*, 932.
(74) Venneman, N. G.; Portincasa, P.; van Berge-Henegouwen, G. P.; van Erpecum, K. J. *Eur. J. Clin. Invest*. **2004**, *34*, 656.
(75) Fuda, E.; Bhatia, D.; Pyle, D. L.; Jauregi, P. *Biotechnol. Bioeng*. **2005**, *90*, 532. Yeang, H. Y.; Yusof, F.; Abdullah, L. *Anal. Biochem*. **1998**, *265*, 381.
(76) Moren, A. K.; Khan, A. *Langmuir* **1995**, *11*, 3636. Moren, A. K.; Eskilsson, K.; Khan, A. *Colloids Surf., B* **1997**, *9*, 305. Moren, A. K.; Khan, A. *Langmuir* **1998**, *14*, 6818.
(77) Moren, A. K.; Khan, A. *J. Colloid Interface Sci*. **1999**, *218*, 397. Moren, A. K.; Regev, O.; Khan, A. *J. Colloid Interface Sci*. **2000**, *222*, 170.
(78) Stenstam, A.; Khan, A.; Wennerström, H. *Langmuir* **2001**, *17*, 7513. Stenstam, A.; Topgaard, D.; Wennerström, H. *J. Phys. Chem. B* **2003**, *107*, 7987. Stenstam, A.; Khan, A.; Wennerström, H. *Langmuir* **2004**, *20*, 7760.
(79) Valstar, A.; Vasilescu, M.; Vigouroux, C.; Stilbs, P.; Almgren, M. *Langmuir* **2001**, *17*, 3208.
(80) Sesta, B.; Gente, G.; Iovino, A.; Laureti, F.; Michiotti, P.; Paiusco, O.; Palacios, A. C.; Persi, L.; Princi, A.; Sallustio, S.; Sarnthein-Graf, C.; Capalbi, A.; La Mesa, C. *J. Phys. Chem. B* **2004**, *108*, 3036.
(81) Moren, A. K.; Nyden, M.; Soederman, O.; Khan, A. *Langmuir* **1999**, *15*, 5480.
(82) Gustavsson, H.; Lindman, B. *J. Chem. Soc., Chem. Commun*. **1973**, 93.
(83) Payne, G. S.; Styles, P. *J. Magn. Reson*. **1991**, *95*, 253.
(84) Wennerström, H.; Lindblom, G.; Lindman, B. *Chem. Scr*. **1974**, *6*, 97.
(85) Lindman, B.; Olsson, U.; Söderman, O. Surfactant Solutions: Aggregation Phenomena and Microheterogeneity. In *Dynamics of Solutions and Fluid Mixtures by NMR*; Delpuech, J.-J., Ed.; Wiley: Chichester, U.K., 1995; Chapter VIII.
(86) Furó, I. *J. Mol. Liq*. **2005**, *117*, 117 and references therein.
(87) Hedin, N.; Furó, I.; Eriksson, P. O. *J. Phys. Chem. B* **2000**, *104*, 8544.
(88) Engström, S.; Jönsson, B.; Jönsson, B. *J. Magn. Reson*. **1982**, *50*, 1.
(89) Hasted, J. B. *Aqueous Dielectrics*; Chapman & Hall: London, 1973; Chapters I−III.
(90) Tauskela, J. S.; Shoubridge, E. A. *Biochim. Biophys. Acta* **1993**, *1158*, 155. Torres, A. M.; Philps, D. J.; Kemp-Harper, R.; Garvey, C.; Kuckel, P. W. *Magn. Reson. Chem*. **2005**, *43*, 217.
(91) Bukhman, Y. V.; Draper, D. E. *J. Mol. Biol*. **1997**, *273*, 1020.
(92) Coppola, L.; Gianferri, R.; Oliviero, C.; Ranieri, G. A. *J. Colloid Interface Sci*. **2003**, *264*, 554.
(93) Magdassi, S.; Vinetsky, Y.; Relkin, P. *Colloids Surf., B* **1996**, *6*, 353.